

# Chapter 3

## Experimental setup

For two reasons most of the measurements presented in this work were performed under ultra high vacuum conditions (UHV). Firstly, the well defined surface of a single crystal is rapidly covered with an adlayer of atmospheric particles <sup>1</sup>. Secondly, as electron spectroscopy is the major tool used in this work UHV conditions are essential for the measurements.

The key tool used for this work was time resolved two photon photoemission spectroscopy. Two femtosecond laser-pulses were used to prepare and probe an electronic state, respectively, where the probe pulse generates a free electron. This electron is detected in a time-of-flight spectrometer and the kinetic energy is determined by means of the flight time.

The first section 3.1 deals with the laser system, in particular with an improved setup for generating ultrashort pulses in the UV developed in part by the author. The second section 3.2 describes the different UHV chambers used during this work for measurements and preparation.

Section 3.3 is concerned with the time of flight spectrometer designed and built by the author for this work.

At the end of the chapter the sample preparation is explained 3.4.

### 3.1 The laser system

The first part of the laser system consists of a commercial Ti:sapphire oscillator combined with a regenerative chirped pulse amplifier setup (Coherent Mira &

---

<sup>1</sup>With a sticking coefficient of one and a base pressure of  $10^{-6}$ mbar a monolayer is deposited in 1s.

RegA 9050) pumped with a 5 W and 10 W Coherent Verdi cw solid state laser, respectively. The recompressed pulses have a bandwidth of 30 nm at 800 nm central wavelength, resulting in 50 fs pulses with a pulse energy of  $8 \mu\text{J}$  at 150 kHz. This pulse is split into two components via a 10:90 beam splitter. The major part is used to drive a noncollinear optical parametric amplifier (NOPA). The rest is sufficient to generate white light, which can either be taken as a probe in transient absorption measurements or can be amplified in a second NOPA setup as described below.

Hitherto, two different types of laser sources were employed for 2PPE measurements. On the one hand high repetition rate laser sources were used, i.e. systems operating at 100 kHz to MHz repetition rate, that deliver fairly long pulses with often limited tunability based on optical parametric amplification (OPA) for frequency tuning or harmonic generation. On the other hand low repetition rate laser sources with repetition rates up to 1 kHz and with a large number of photons per pump pulse were employed. The latter systems render slow signal accumulation, however the superior noncollinear optical parametric amplification (NOPA) technology [117, 118] can provide extremely short and highly tunable pulses. Recently, tunable sub-20 fs ultraviolet pulses have been achieved with appropriate chirp management in the visible [119].

When we decided to use a noncollinear OPA, commercial setups were available only for 1 kHz amplified systems with a much higher pulse energy. We had to

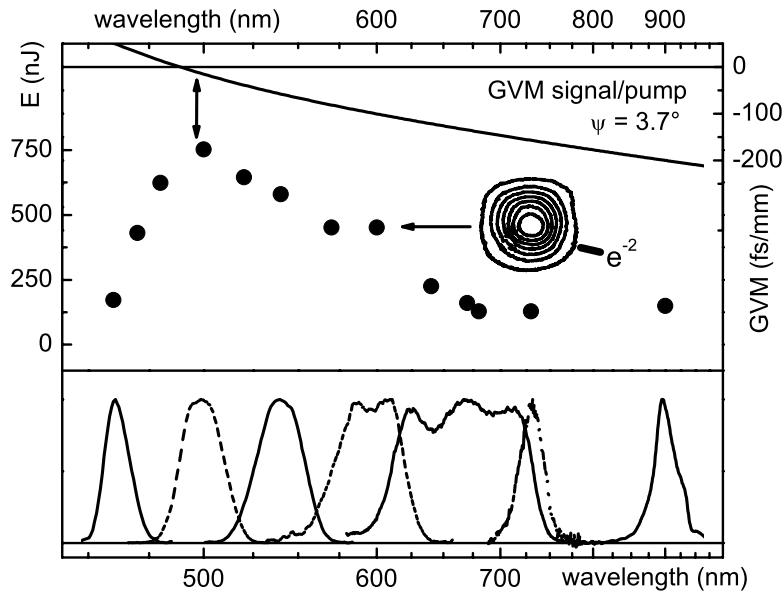


Figure 3.1: Output energy and spectra. The spatial mode is shown in the inset and the group velocity mismatch between the 400 nm pump light and the visible signal is given at the top of the figure for a non-collinearity of  $3.7^\circ$ .

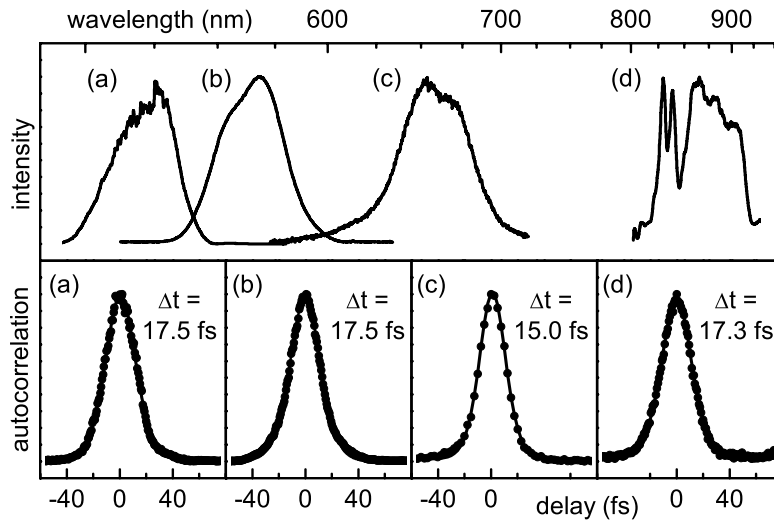


Figure 3.2: Spectra and intensity autocorrelation traces (together with the sech2-fit pulse width) for pulses at four different central wavelengths.

adopt the known setup to our pulse energies. This was done in collaboration with the group of Prof. Riedle at the LMU Munich who were among the first groups using and developing the NOPA technology [117]. It turned out that the 100 kHz NOPA required a significant change in the beam profile to generate the desired intensity of 100 GW/cm<sup>2</sup> inside the BBO crystal. Details of this setup (upper part of Fig. 3.4) are described in Ref. [120]. Output power, group velocity mismatch between signal and pump pulse and the beam profile for different wavelength are shown in Fig. 3.1. Characteristic autocorrelation traces at different wavelengths are shown in Fig. 3.2.

As shown in section 2.6.1.1 the first optical transition of the molecule under investigation, i.e. perylene, takes place at about 440 nm. This spectral region is not accessible with a NOPA pumped at 400 nm, because the required idler wavelength would be 4.4  $\mu$ m where BBO is strongly absorbing. Instead, we generated 880 nm pulses with a typical spectral width of < 70 nm and frequency doubled these pulses in a SHG setup [121]. It is convenient to compress the pulse prior to the SHG processes [122]. By carefully fine tuning this setup we generated 440 nm pulses with a spectral width of 25 nm, resulting in a temporal Fourier limit of sub 10 fs. With a standard silica prism compressor these pulses were compressed down to 13 fs. Typical spectra and autocorrelation traces for 870-435 nm SHG output are shown in Fig. 3.3.

As mentioned before, a second pulse in the UV is necessary for the 2PPE measurements to emit the electrons from the sample. A common method for this is frequency tripling the fundamental wavelength. Due to the very limited

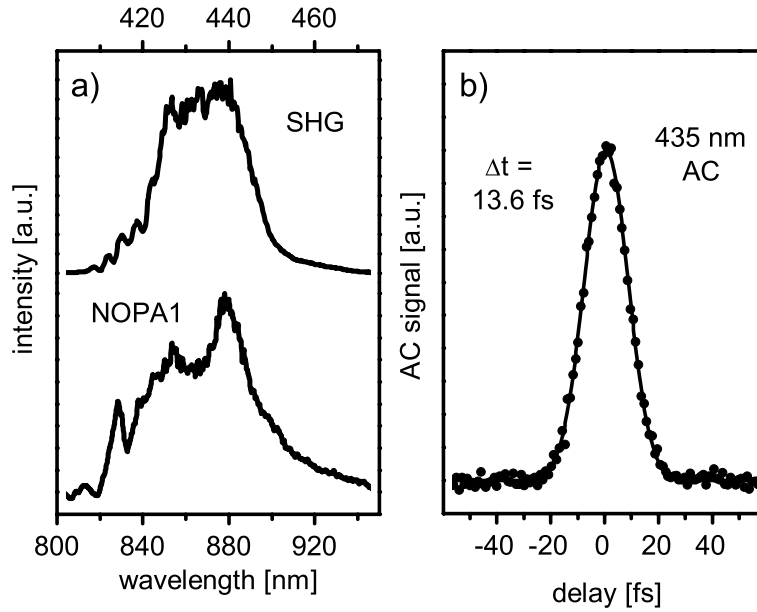


Figure 3.3: (a) Fundamental and SHG spectra for 865/435 nm pulses. (b) Auto-correlations are shown for 435 nm together with fitted Gaussian and FWHM.

angular acceptance of the BBO crystal in the UV this results in a narrow band width and thus long pulse. Because of that I decided to build a second NOPA and frequency double the visible output. As the output power of our regenerative amplifier was insufficient to drive two NOPAs at the same time the remaining 400 nm pump pulse of the first NOPA was used a second time together with a second white light setup. It turned out that the spectral width achievable with this setup was comparable to that of the first NOPA.

The setup for the second NOPA is shown inside the dashed box in Fig. 3.4. The residual 400 nm light not used in the first NOPA process was recollimated with lens L (focal length: 20 cm) and focused with the concave mirror M (radius of curvature: 37.5 cm). The 2 mm BBO crystal was placed in the focal plane of M where pump pulse and white light continuum overlapped with an internal angle of about  $\pm 3.7^\circ$ . As the 400 nm pump pulse was reduced in power and the spatial mode was slightly distorted due to the first conversion process, the second NOPA yielded less pulse energy than the first. Typically NOPA1 generated pulse energies of about 100 nJ in the NIR where usually lower output is observed [54, 120], NOPA2 100 nJ in the visible. The spectral width and the compressibility (Fig. 3.5) were quite comparable to the first setup.

The subsequent SHG process results in pulses with a spectral width ranging from 6 nm at 250 nm to 12 nm at 320 nm. These pulses can be compressed to sub-20 fs width (Fig. 3.5).

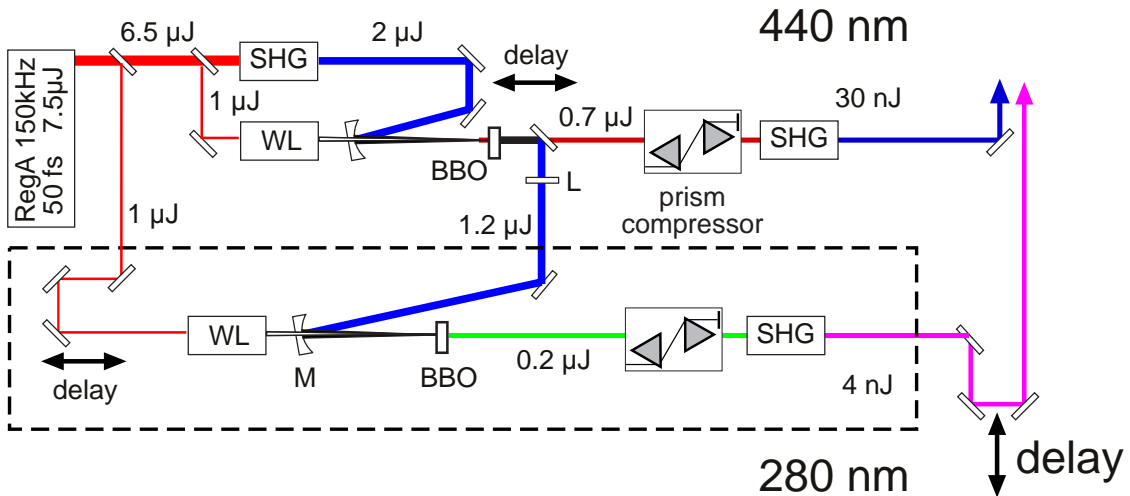


Figure 3.4: Setup for two 150 kHz NOPAs pumped with one 400 nm SHG pulse. The second NOPA is shown inside the dashed box. See text for details.

The visible output of the first NOPA is limited by the second order chirp

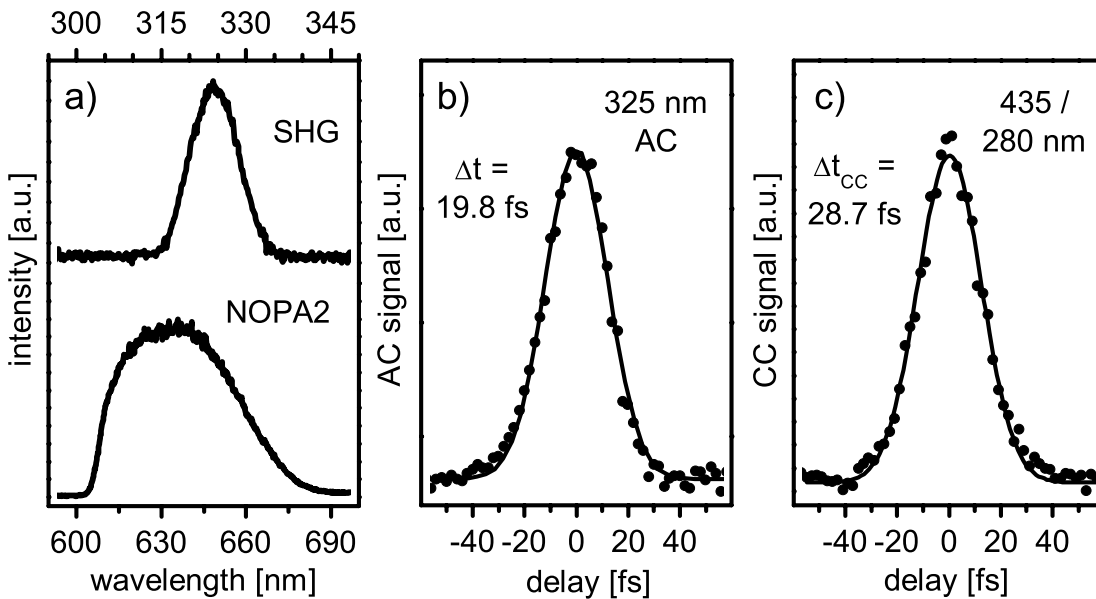


Figure 3.5: NOPA2: (a) Fundamental and SHG spectra for 640/325 nm pulses. (b) Autocorrelation shown for 325nm. (C) Crosscorrelation of 435 nm and 280 nm pulses (together with fitted Gaussian and FWHM).

and may be compressed further by inserting a deformable mirror in the prism compressor to account for higher order chirp as shown in Ref. [57]. In contrast, the UV pulse of the second setup is mainly limited due to the narrow angular acceptance of the BBO crystal at this wavelength. It is possible to circumvent

the latter limitation by achromatic SHG, where different spectral components are focused with different angles into the nonlinear crystal [123]. This is a promising possibility for future work.

## 3.2 Ultra-high vacuum chambers

A major prerequisite for this work was to combine surface science tools for investigating the interface with wet chemistry procedures for preparing the interface. So far, research on adsorbate covered surfaces has been carried out mostly on atoms or relatively small molecules attached to well defined single crystal surfaces with surface science techniques (e.g. PES, LEED, STM) or on colloidal systems (films or solutions) with electro-chemical or (electro-)optical techniques. In the former case clean single surfaces are usually prepared by sputtering and/or heating, cleaving or epitaxial growth in MBE or MOCVD facilities. To prevent contamination of the surface the adsorbate is evaporated in an UHV chamber. This preparation procedure is restricted to molecules that can be evaporated without undergoing fragmentation. The organic compounds for example used in this work can not be easily evaporated.

In the latter case the use of colloidal systems is necessary because of the restricted sensitivity of the experimental techniques. Whereas even huge, fragile molecules can be used as long as they can be brought in solution, cleanness of the colloidal surfaces and the binding geometry of the molecules are less defined compared to single crystal surfaces.

For a systematic investigation of the influence of specific molecular properties on heterogeneous electron transfer it is advantageous to vary properties of the molecules by systematic chemical tailoring. A variety of perylene derivatives have been synthesized by our group in recent years (see Sec. 2.6.1). To investigate interfacial ET of these molecules with surface science techniques, especially TR-2PPE, on well defined single crystal surfaces, a special preparation procedure was developed in this work where the substrate was cleaned under UHV conditions and was coated via adsorption of the molecules from solution in a special UHV chamber. In this chamber it was possible to switch between UHV condition and an inert-gas atmosphere. This way molecules can be adsorbed from solution with a minimum chance of contamination.

All UHV chambers that are used in our group are equipped with load-lock ports allowing for contamination-free transport between different UHV chambers via a

mobile UHV chamber [124]. Three UHV chambers were used for this work:

### 3.2.1 Measurement chamber

A separate UHV chamber was used for the TOF-measurements and for UHV-preparation, respectively. The first chamber was equipped with a home built time of flight spectrometer (see Sec. 3.3) and a liquid helium cryostat for cooling the samples down to 20 K. The UHV-preparation chamber was equipped with an ion gun for  $\text{Ar}^+$  ion bombardment and a specific sample holder for heating the sample via resistivity heating. The two UHV chambers were connected via a valve.

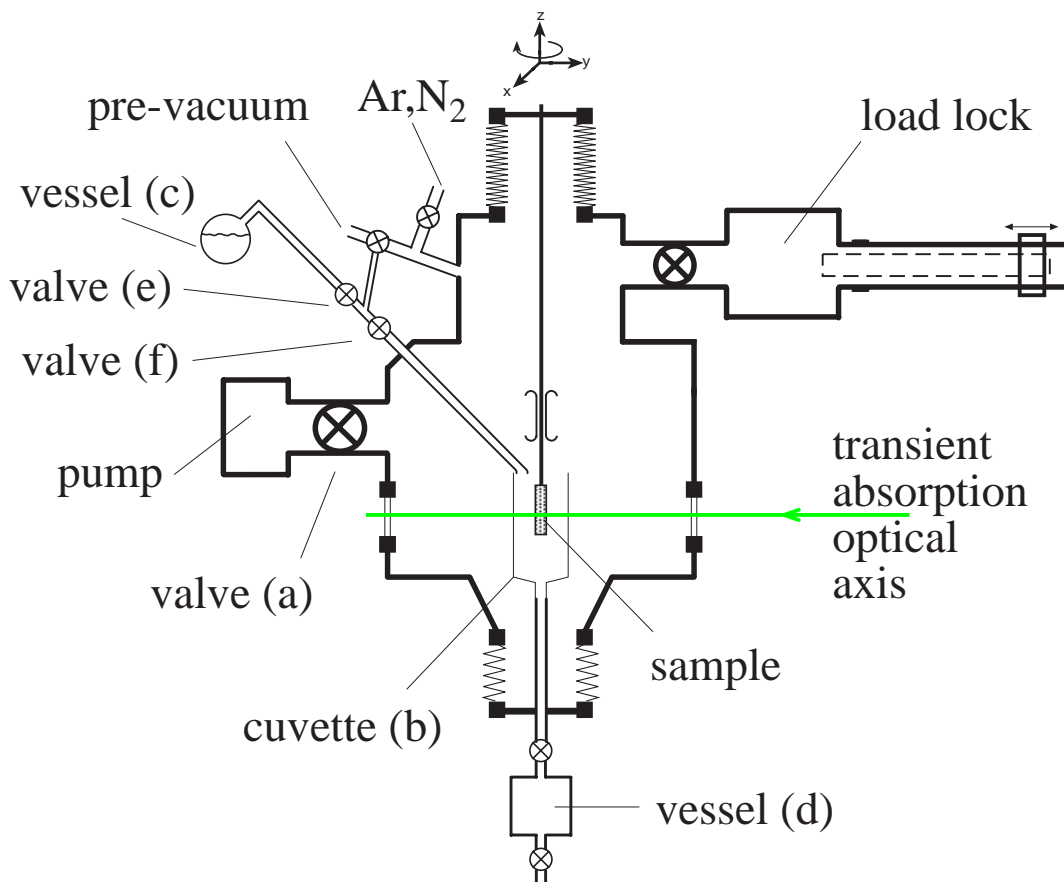


Figure 3.6: Preparation chamber

### 3.2.2 Preparation and transient-absorption chamber

The preparation chamber for adsorbing molecules from solution (pat. pending) was designed by R. Ernstorfer and is described in detail in [64]. The chamber was built firstly with the goal to switch between UHV, an inert gas, and a liquid environment. This UHV chamber was also designed for carrying out transient absorption measurements. A second application is the usage as a preparation chamber. The chamber (Fig. 3.6) was equipped with the valve (a) between a CF-100 turbomolecular pump and the main chamber. It was closed prior to flooding the chamber with 5.0 argon or nitrogen, purified by a double stage purifier (Oxisorb, Messer Griesheim). Under inert gas conditions the cuvette (b) fixed on the bottom of the chamber was filled with a solvent prepared in a vessel (c) and emptied in another vessel (d) by changing the Argon pressure in the main chamber and opening the respective valves. When the preparation procedure was finished the chamber was first evacuated by a pre-vacuum pump to  $10^{-3}$  mbar and then, by opening valve (a), with the turbomolecular pump to  $10^{-9}$  mbar. A detailed description of the interface preparation is given in Sec. 3.4.

In addition this chamber was equipped with UHV windows to allow for transient absorption measurements. The entrance window was specifically designed to minimize the dispersion of the laser pulses. The window is only 140  $\mu\text{m}$  thick. The description of construction details is given in Ref. [64].

### 3.2.3 ESCA chamber

The ESCA (Electron Spectroscopy for Chemical Analysis) chamber was equipped with a hemispherical electron analyzer (VSI, HSA100) a gas discharge lamp (Spex UVS10/35) for UPS measurements, a double anode (Mg,Al) X-ray source (Spex RQ20/38) for XPS measurements, and a LEED facility (Spex). It turned out that the hemispherical electron analyzer showed malfunctions. Whereas the relative peak positions were reliable, the absolute positions were not (e.g. unrealistic band gaps of more than 3.5 eV were measured on  $\text{TiO}_2$ ). Charging of the samples could be excluded because the samples showed sufficient conductivity (Sec. 4.1.1) and no charging effects were observed in 2PPE measurements, not even at 30 K. UPS spectra for this work were recorded with excitation by HeI emission at 21.22 eV. XPS spectra were measured by using the  $\text{MgK}_\alpha$  line (1253.6 eV) for excitation.



### 3.3 Time of flight spectrometer

For the present work a new time-of-flight (TOF) electron spectrometer was designed and constructed (Fig. 3.7). The zero-kinetic-energy TOF (ZEKE-TOF) used in our group before was not suited for angular resolved measurements because the ZEKE setup requires a set of plane apertures at the entrance of the TOF. These plane apertures hindered the angular positioning of the sample in front of the entrance. Therefore, the entrance aperture was formed as a cone with opening angle of  $25^\circ$ . The cathode grid was made from thin molybdenum wires with a diameter of only 0.1 mm. The overall drift length between entrance and cathode was 313 mm resulting in an angular acceptance of  $\pm 7.3^\circ$ . Drift tube, entrance aperture and cathode grid were coated with carbon to achieve a homogeneous potential inside the drift tube. The drift tube was isolated against the vacuum flange and a bias potential could be applied between sample and drift tube. The cathode was followed by two micro channel plates (MCP) twisted against each other by  $90^\circ$ . The electron cascade from the last MCP was collected by a plane anode and coupled out via a vacuum compatible capacitor. The overall potential between cathode and anode was 3 kV.

The signal from the capacitor was amplified by an *Ortec VT 120 FastPreamp* and fed into a constant fraction discriminator *Ortec 934 Quad CFD*. The NIM output from the CFD was delayed in an *Ortec 425A Delay* and processed in an *Ortec 9308 picosecond TimeAnalyzer*. The time analyzer was replaced at the same time as the TOF. Therefore, a new measurement software was implemented using LabView. The conversion from time-of-flight to kinetic energy was implemented in the program as well as the control of the delay stages, application



Figure 3.7: The new time of flight spectrometer

of the bias potential via a National Instruments DA converter and an external trigger for the time analyzer.

The time analyzer was operated in single-shot mode. The system cannot process more than one emitted electron for each laser pulse. In the case of two emitted electrons, only the first one would be processed and this will privilege the detection of high energy electrons. To prevent a distortion of the spectrum the count-rate was limited to 1% of the repetition rate of the laser.

The typical distance between sample and entrance aperture was 1 mm. In principal, for measurements with an applied bias between sample and TOF, this acceleration distance enters the equation for conversion from time-of-flight to kinetic energy. It turned out that at least for bias potentials below 1 V no differences can be observed when the acceleration step is neglected in the conversion procedure. Neglecting the acceleration step is equivalent to the assumption that the electron gains the kinetic energy instantaneously from the applied potential and has constant velocity even along the short distance between sample and entrance aperture. This has the advantage that the conversion can be carried out analytically in real-time during the measurement.

The main output format of the program was a binary matrix containing counts vs. time delay and kinetic energy. For data analyzing separated programs were developed allowing background subtraction, simple arithmetic manipulations between matrices, the extraction of time traces (energy spectra) by integrating over variable energy (time delay) ranges and the conversion in ASCII format.

For angular-resolved measurements the output was an ASCII file containing the uncorrected flight times. The conversion into kinetic energy and simple arithmetic operations were implemented in  $C^{++}$ .

Routines for data fitting by means of optical Bloch equations, rate models and

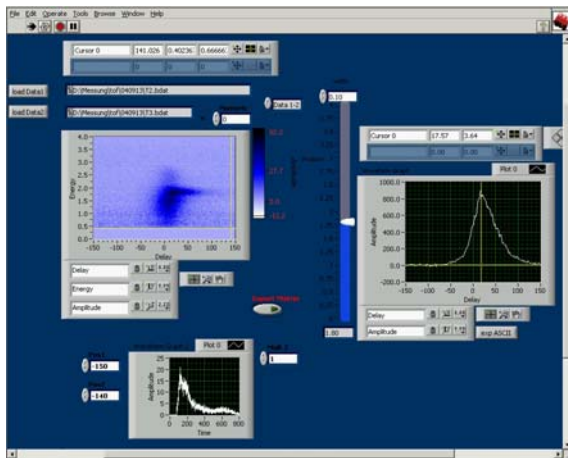


Figure 3.8: GUI of one of the data processing tools.

Fresnel equations were implemented in Maple using a multidimensional downhill simplex minimization method [125].

The TOF setup was carefully tested for various bias potentials by measuring the energetic position and the dispersion of image potential states on the Cu(111) surface and comparing the results with the ones measured with the formerly used TOF and with published data [126]. Time-resolved measurements are discussed in detail in Sec. 4.2.1.

## 3.4 Sample preparation

### 3.4.1 Colloidal TiO<sub>2</sub> films

The colloidal films used for transient absorption measurements were prepared following Grätzel et al. [5, 127]. Nano-porous 2  $\mu\text{m}$  thick layers composed of anatase nano-particles of 15 nm diameter on average with about 50% space filling, and (101) as the dominating surface plane were prepared. Coating with the dyes and characterization of the samples are described in detail in [64]. Briefly, the colloidal films were heated up to 450 °C in laboratory air and cooled down to room temperature under argon atmosphere. The investigated perylene dyes were adsorbed on the colloidal film by immersing the latter in a  $10^{-4}$  M solution of the respective perylene dye in toluene for 5-20 min at room temperature. This resulted in an absorbance of 0.5-0.8 OD at 440 nm. The dye-covered TiO<sub>2</sub> electrode was rinsed with dried solvent, dried under argon atmosphere, and transferred to UHV.

### 3.4.2 Rutile TiO<sub>2</sub>(110) single crystals

Rutile (110) oriented single crystals were purchased from CrysTec, Berlin with the dimension 10x10x0.5 mm<sup>3</sup>. The average roughness of the crystals was typically below 0.1nm. Two crystals were mounted on one sample holder, made of molybdenum, and fixed with two molybdenum clamps. The sample holder was equipped with a tungsten wire for resistivity heating and a Ni/CrNi thermocouple. To obtain a reference sample both crystals were mounted with the [001] axes parallel, for measuring the binding geometry of the molecules by means of AR-2PPE, the crystals were mounted with the [001] axes perpendicular to each other. The orientation of the crystals was measured via LEED.

The samples were cleaned by Ar<sup>+</sup> ion bombardment (700 eV, 5  $\mu\text{A}$ , 10 min) and

subsequent annealing (875 K, 10 min). Characterization of the cleaned samples is described in Sec. 4.1.1. After 4 cycles of above mentioned cleaning procedure had been completed the samples were transported via a mobile UHV chamber ( $5 \cdot 10^{-10}$  mbar) to the solvent chamber.

### 3.4.2.1 Coating the surface with molecules

The solutions with the molecules were prepared as follows: The amount of dye necessary for preparing a 0.1 mM solution was weighed and brought into a special glass vessel attached to a CF-20 flange. The vessel was attached to a distiller filled with methanol and potassium as drying agent. The whole apparatus was sealed with Teflon gaskets and connected via valves to a rotary vacuum pump and a nitrogen inlet. With the glass vessel attached the apparatus was evacuated and baked out with a hairdryer. The apparatus was partially filled with nitrogen and the distilled and dried solvent was sucked into the vessel. The same procedure was repeated with a distiller containing toluene to obtain a solvent composed of 25% methanol and 75% toluene. Afterwards the vessel was filled with nitrogen, the valve was closed and the vessel was connected to the solvent chamber.

The tube between the two valves e and f(Fig. 3.6) was evacuated via the pre-vacuum pump and baked out with a hot-airgun. The sample was brought into the chamber and valve a was shut. The chamber was filled with nitrogen to approximately 600 mbar, well below the pressure inside the flask, and the solution was sucked into the cuvette. The sample was immersed into the solution. To have a reference sample only the lower of the two crystals was immersed, whereas in the case of AR-2PPE measurements, both samples were dipped into the solution. After 30 min the chamber was filled with nitrogen to about 1050 mbar and the solution was pressed into the other vessel (d). In the mean time pure solvent was prepared in the same way as described for the solution. The sample was rinsed three times by immersing it into the pure solvent the same way as already described for the solution. During the last cleaning cycle even the reference sample was dipped into the solvent in order to correct for possible solvent residues on the sample. Afterwards the chamber was evacuated via the pre-vacuum inlet and then pumped down to  $3 \cdot 10^{-9}$  mbar by opening valve (a) over night.

### 3.4.3 Copper and silver single crystals

Copper and silver single crystals were purchased from MaTeck. They were mounted on a sample holder via two tungsten wires that fit into two slits on both sides of the crystals. Additionally, the wires were used to heat the samples by resistivity heating. A Ni/CrNi thermocouple was electrically insulated by a glass coating and inserted into a hole drilled in the crystal.

The samples were cleaned by Ar<sup>+</sup> ion bombardment (500 eV (Cu), 500 eV (Ag), 5  $\mu$ A, 10 min) and subsequently annealing (750 K (Cu), 700 K (Ag), 10 min). Characterization of the cleaned samples is described in Sec. 4.1.2. For samples which had been exposed for some time to air, several cycles of sputtering and annealing were necessary. For the Cu (111) crystal, that was routinely used for cross-correlation measurements, one cycle was sufficient for day by day cleaning. The procedure for adsorption of the molecules was the same as for the rutile TiO<sub>2</sub> single crystals.